

Vec2Face-v2: Unveil Human Faces from their Blackbox Features via Attention-based Network in Face Recognition

Thanh-Dat Truong^{1†}, Chi Nhan Duong², Ngan Le¹, Marios Savvides³, Khoa Luu¹

¹*CVIU Lab, University of Arkansas, Fayetteville, USA*

²*Department of Computer Science and Software Engineering, Concordia University, Canada*

³*Carnegie Mellon University, USA*

{tt032, khoaluu, thile}@uark.edu, dcnhan@ieee.org,
marios@andrew.cmu.edu

Abstract

In this work, we investigate the problem of face reconstruction given a facial feature representation extracted from a blackbox face recognition engine. Indeed, it is very challenging problem in practice due to the limitations of abstracted information from the engine. We therefore introduce a new method named Attention-based Bijective Generative Adversarial Networks in a Distillation framework (DAB-GAN) to synthesize faces of a subject given his/her extracted face recognition features. Given any unconstrained unseen facial features of a subject, the DAB-GAN can reconstruct his/her faces in high definition. The DAB-GAN method includes a novel attention-based generative structure with the new defined Bijective Metrics Learning approach. The framework starts by introducing a bijective metric so that the distance measurement and metric learning process can be directly adopted in image domain for an image reconstruction task. The information from the blackbox face recognition engine will be optimally exploited using the global distillation process. Then an attention-based generator is presented for a highly robust generator to synthesize realistic faces with ID preservation. We have evaluated our method on the challenging face recognition databases, i.e. CelebA, LFW, AgeDB, CFP-FP, and consistently achieved the state-of-the-art results. The advancement of DAB-GAN is also proven on both image realism and ID preservation properties.

Keywords: Vec2Face-v2, Vec2Face, Bijective Metric Learning, DiBiGAN, DAB-GAN, Knowledge Distillation, Transformers

1. Introduction

Face recognition [1] has recently matured and achieved remarkable accuracy against the large number of classes. There have been many approaches proposed in literature

[†]Corresponding Author

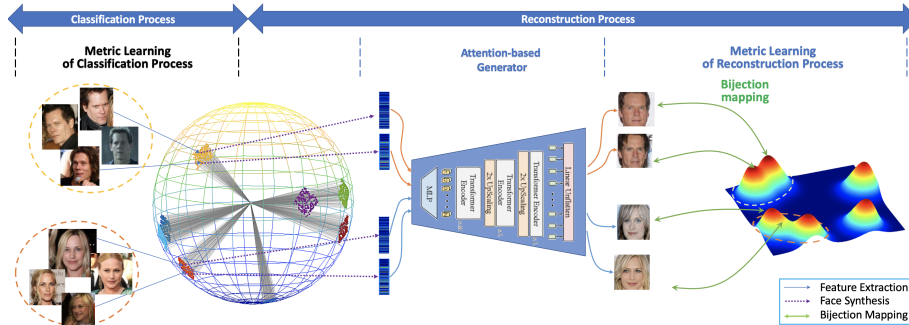


Figure 1: **Metric Learning for Image Reconstruction.** By maintaining the one-to-one mapping via a bijection, the distance between images can be directly and intuitively measured and enhances the metric learning process for image reconstruction task.

which can be divided into two groups: i.e. “*closed-set*” and ‘*open-set*’ image recognition. While the first group aims at recognizing only classes that are seen from training data, the second group relaxes the constraint on predefined classes and provides more power to recognize classes that are not included in its training data. A typical *open-set* recognition system is designed in two main phases, i.e. feature extraction, and feature comparison. The role of feature extraction is more important since it directly determines the robustness of the engine. This operator defines an embedding process mapping input facial images into a higher-level latent space where embedded features extracted from photos of the same subject distribute within a small margin. Moreover, to protect the technologies, most recognition systems are usually set into a *blackbox* mode before their deployment stage. Therefore, in terms of both “*blackbox*” and “*open-set*” criteria, there are limited apparent attempts to inverse that embedding process for reconstructing input images of a subject given the extracted features from those *blackbox* recognition engines. We refer this as a “*feature reconstruction*” problem.

Some Adversarial Attack approaches [2, 3, 4, 5, 6] have partially addressed this task in the form of analyzing the gradients of recognition engine’s outputs to generate adversarial examples that mislead the recognition engines’ behaviours. Either in the context of whitebox or blackbox modes, these approaches are usually limited their working domain of predefined classes from training set of the recognition engines. More importantly, the ultimate goal of these approaches are to generate imperceptible perturbations (i.e. random patterns) to be added to given input signals rather than synthesizing new images from scratch. Other methods [7, 8, 9, 10, 11] to reverse the process of feature extraction from classification models and to explain the actual “knowledge” embedded in these models are also introduced in literature. Although they can directly produce images without prior inputs as previous approaches, their crucial assumption is that the classifier structure is accessible, i.e. whitebox setting. Meanwhile, our goal focuses on a more challenging reconstruction task with a *blackbox* recognition model. Firstly, this process *reconstructs faces from scratch* without any hint from input images. Secondly, in a blackbox setting, there is *no information about*

Table 1: Comparisons of our DibiGAN and other unrestricted synthesis methods. Image Reconstruction (Img_Recon), Feature Representation (Feat), Guided Image (Img_G), Feature Conditional (Feat_Cond), Neighborly Deconvolution (NB_Deconv), Optimization (Opt), Face Recovery (FaRe), Zero-order Optimization (ZO-Opt), Auto-Encoder (AE).

	Ours	GMI [12]	FaRe [13]	NBNet [14]	SynNormFace [8]	IFaceRec [11]	INVREP [15]
Input	Feat						
Signal Type	Face/Human Body	Face	Face	Feat Face	Feat Face	Feat + Img _G Face	Feat Face
Feature Type	CNN-based			CNN-based	CNN-based	CNN-based	CNN-based
Generator Structure	Feat_Cond	AE	ZO-Opt	NB_Deconv	MLP + CNN	DeConvNet	Opt
Blackbox Support	✓	✗	✓	✓	✗	✗	✗
Img_Recon Metric	Bijjective	✗	✗	✗	✗	✗	✗
Exploited Knowledge from Classifier	Fully (Distillation)	Partially	Fully (Whitebox)	Partially	Fully (Whitebox)	Fully (Whitebox)	Fully (Whitebox)

the engine’s structure, and, therefore, it is unable to directly exploit knowledge from the inverse mapping process (i.e. back-propagation). Thirdly, the embedded features from a recognition engine are for *open-set problem* where no label information is available. More importantly, the subjects or classes to be reconstructed may have never been seen during training process of the recognition engine.

In the scope of this work, we assume that the recognition engines are primarily developed by deep Convolutional Neural Networks (CNN) that dominate recent state-of-the-art results. We also assume that there is no further post-processing after the step of CNN feature extraction. This paper presents a novel generative structure, namely Attention-based Bijjective Generative Adversarial Networks in a Distillation framework (DAB-GAN), with Bijjective Metric Learning for the image reconstruction task. Far apart from previous approaches where the introduced metrics mainly fulfill the discriminative criteria of classification process, the proposed Bijjective Metric Learning with bijection (one-to-one mapping) property provides an more effective, natural way to measure the distance between images for image reconstruction task. A preliminary version of our work can be found in [16]. In that work, the proposed DiBiGAN with Bijjective Metric are able to synthesize faces with wide range of in-the-wild variations against different face matching engines and demonstrate the advantages on synthesizing realistic faces with subject’s visual identity. In this paper, we further exploit the effect of the generator to the synthetic results. In particular, although convolution-based generator has achieved remarkable performance, it still remain some issues related to long-range dependencies. Also, the CNN-based generator is limited to model the complex patterns and structure. Therefore, to further improve the robustness and reliability our DAB-GAN, we propose an attention-based generator designed based on Transformers. As a result, the model represented in this work is more advanced in terms of the synthesizing capability of our attention-based generator. In summary, the contributions of this work are five-fold.

- A novel parametric metric, i.e. ***Bijjective Metric***, for the *feature reconstruction* task is presented. By analyzing limitations of common metrics in feature reconstruction, i.e. non-parametric (e.g. ℓ_p) and parametric metric (e.g. classifier-based metric), we propose a novel ***Bijjective Metric Learning*** with bijection (one-to-one mapping) property so that the distance between latent representations in the latent space are equivalent to the distance those images. Therefore, our proposal provides a more effective and natural metric learning approach to the fea-

ture reconstruction problem.

- We introduce a novel *Attention-based Generator* that is purely designed based on the Transformer architecture. The novel attention-based generator is able to capture the global and local information and model the complex visual structures.
- *Different aspects of the distillation process* for the image reconstruction task in a blackbox mode are also exploited. They include distilled knowledge from the blackbox image recognition and ID knowledge extracted from a real structure of the object or subject.
- A *Feature-conditional Generator Structure* learned by *Exponential Weighting Decay Strategy* within a Generative Adversarial Network (GAN)-based framework is introduced to improve the robustness of the generator to synthesize realistic images with identity preservation.
- The *intensive evaluations on face recognition benchmarks* have showed the performance of our proposal in both image realism and identity preservation.

To the best of our knowledge, this is one of the first metric learning methods for image reconstruction (Table 1). The paper is organized as follows. Section 2 reviews some recent approaches to synthesize images from given (deep) features and Transformer backgrounds. Section 3 presents the feature reconstruction problem w.r.t. blackbox image recognition engines and the proposed network architecture. Then, we analyze choices of available metrics being adopted and their limitations followed by proposing a novel bijective metric. Then, different aspects of the distillation process and the proposed Generator Structure of DAB-GAN for the image reconstruction task in a blackbox mode are also exploited and formulated. Finally, the experimental results together with conclusion are given in Sections 6. and 7.

2. Related Work

Synthesizing images from their deep features has brought several interests from the community. According to the motivations and approaches to be used, they can be divided into two groups, i.e. unrestricted and adversarial synthesis methods.

2.1. Unrestricted Synthesis Methods

The approaches in this direction focus on reconstructing an image from scratch given its high-level representation. Since the mapping is from a low-dimensional latent space to a highly nonlinear image space, several regularizations have to be applied, e.g. Gaussian Blur [17] for high-frequency samples or Total Variation [15] for maintaining piece-wise constant patches. These optimization-based techniques are limited with high computation and unrealistic reconstructions. Later, Dosovitskiy et al. [9] proposed to reconstruct the image from its shallow (i.e. HOG, SIFT) and deep features using a Neural Network (NN). Zhmoginov et al. [11] presented an iterative method to invert Facenet [18] feature with feed-forward NN. Cole et al. [8] proposed an auto-encoder structure to map the features to frontal neutral face of the subject. Yang et al.

[19] also adopted autoencoder for model inversion task. Generally, to produce better synthesized quality, these approaches require full access to the deep structure to exploit the gradient information from the embedding process. Mai et al. [14] developed a neighborly deconvolutional network to support the blackbox mode. However, with only pixel and perceptual [20] losses, there are limitations of ID preservation when synthesizing different features of the same subject. In this work, we further address and solve this issue using Bijective Metric Learning and Distillation Knowledge for the reconstruction task.

2.2. Adversarial Synthesis Methods

Rather than reconstructing the images from scratch, Adversarial approaches aim at generating unnoticeable perturbations from input images for adversarial examples to mislead the behaviour of a deep structure. Either directly accessing or indirectly approximating gradients, adversarial examples are created by maximize corresponding loss which can fool a classifier [7, 21, 22, 2, 3, 23, 24, 25, 4]. Ilyas et. al. [3] proposed bandit optimization to exploit prior information about the gradient of the deep learning models. Later, Ilyas et. al. [2] introduced Natural Evolutionary Strategies to enable query-efficient generation of black-box adversarial examples. Other knowledge from the blackbox classifier are also exploited for this task [4, 7, 10]. Generally, although the approaches in this direction tried to extract the gradient information from a blackbox classifier, their goal is mainly to mislead the behaviours of the classifier with respect to a pre-defined set of classes. Therefore, they are closed-set approaches. Meanwhile, in our work, the proposed framework can reconstruct faces of subjects that have not been seen in the training process of the classifier.

2.3. Transformer Background

Transformer is initially used to Natural Language Processing (NLP) tasks, where it has demonstrated considerable progress [26, 27, 28]. Vaswani et al. [26], for example, were the first to propose a transformer based on an attention mechanism for machine translation and English constituency parsing tasks. Devlin et al. [27] proposed a novel language representation model called BERT (short for Bidirectional Encoder Representations from Transformers), which pre-trains a transformer on unlabeled text while accounting for each word's context (it is bidirectional). BERT achieved state-of-the-art performance on NLP tasks. Brown et al.[28] used 45 TB of compressed plaintext data to build a huge transformer-based model termed GPT-3 (short for Generative Pre-trained Transformer3) with 175 billion parameters. It delivered strong results on a variety of downstream natural language tasks without the need for fine-tuning. These transformer-based models, with their high representation capacity, have made substantial advances in NLP.

Researchers have lately adapted transformer to computer vision (CV) applications, inspired by the significant success of transformer designs in the field of NLP. CNNs are regarded the core component in vision applications [29, 30], however a transformer is currently showing promise as a viable replacement to CNN. ViT is another vision transformer model that applies a pure transformer directly on picture patch sequences. Dosovitskiy et al. [9] recently suggested it, and it has achieved state-of-the-art performance on various image recognition benchmarks. Transformer has been used to solve

a range of different computer vision issues, including object identification [31, 32], semantic segmentation, image processing, and video comprehension, in addition to simple image classification. Because of its superior performance, an increasing number of academics are proposing transformer-based models for enhancing a wide range of visual tasks.

Transformer For Image Reconstruction Jiang et al. [33] introduced GAN architecture that consists of generator based on transformer to improve the resolution of features and a discriminator to obtain the low-level textures and semantic contexts. They also introduced a novel module of self-attention that improves the memory bottleneck to enhance the high-resolution generation. Lin et al. [34] introduced GAN architecture which utilizes spatial transformer network(STN), which operated in the geometric warp parameter space. They proposed a sequential training strategy and an iterative STN warping scheme which proved better than the training of a single generator. Hudson et al. [35] introduced a network which has a bipartite structure that maintains linearly efficient computation, this iteratively propagates information to support the refinement of images. This method uses multiplicative integration which eases the region-based modulation. Esser et al. [36] proved the efficient way of combining CNNs with the transformers to synthesize high-resolution images. They showed how CNNs are used to learn the context of the images and use the transformers to efficiently model the composition in the high-resolution images. Chen et al. [37] trained a sequential transformer which predicts the pixels auto-regressively and this whole procedure is done without the knowledge of inputs.

3. Feature Reconstruction Problem

In this section, we detail the feature reconstruction problem in face recognition. First, the formulation in this problem will be mathematically defined. Then, the proposed network architecture will be introduced using CNN-based generator and Attention-based generator.

3.1. Problem Formulation

Given an input image \mathbf{I} in the image space $\mathcal{I} \in \mathbb{R}^{H \times W \times 3}$ (H, W are the height and width), a function $F : \mathcal{I} \rightarrow \mathcal{F}$ maps an input image $\mathbf{I} \in \mathcal{I}$ to its deep feature representation space $\mathcal{F} \in \mathbb{R}^M$ (M is the feature dimension length). An additional function $C : \mathcal{F} \rightarrow \mathcal{Y}$ takes the deep feature $F(\mathbf{I})$ as an input and produce the the corresponding identity prediction of the subject in the space $\mathcal{Y} \in \mathbb{R}^N$ where N is the number of predefined subject classes in the training dataset. Two types of reconstruction problem can be defined as follows.

Definition 1. Model Inversion: Given blackbox functions F and C ; and a prediction identity vector \mathbf{s} extracted from an unknown image I , i.e. $\mathbf{s} = [F \circ C](\mathbf{I})$, the model inversion task will recover an input image \mathbf{I} from \mathbf{s} such that

$$\tilde{\mathbf{I}}^* = \arg \min_{\tilde{\mathbf{I}}} \mathcal{L}([F \circ C](\tilde{\mathbf{I}}), \mathbf{s}) \quad (1)$$

where \mathcal{L} defines some types of distance metrics.

The approaches to the model inversion problem can be addressed by exploiting the relation between the input image and its class label. Additionally, the number of classes N is predefined by the number of training subject identities, the model inversion is limited to images of the training sets. The problem in this case is also known as the *closed-set reconstruction*.

Definition 2. Feature Reconstruction: Given a blackbox function F ; and its embedding feature $\mathbf{f} = F(\mathbf{I})$ of an unknown image \mathbf{I} , feature reconstruction is to recover \mathbf{I} from \mathbf{f} by optimizing Eqn. (2) as follows,

$$\tilde{\mathbf{I}}^* = \arg \min_{\tilde{\mathbf{I}}} \mathcal{L}(F(\tilde{\mathbf{I}}), \mathbf{f}). \quad (2)$$

Different from the first type, this problem relaxes the constraint on the number of classes, making it an *open-set reconstruction* problem. This brings more challenging factors to the reconstruction process as the target reconstructed faces are not necessary to be seen by F during its training process. Moreover, as parameters of F is inaccessible, gradient-based approaches [38] have become infeasible. A solution for this task is to learn a reverse mapping function of F , i.e. *generator*, $G : \mathcal{F} \rightarrow \mathcal{I}$ as in Eqn. (3).

$$\begin{aligned} \tilde{\mathbf{I}}^* &= G(\mathbf{f}; \theta_g) \\ \theta_g &= \arg \min_{\theta} \mathbb{E}_{\mathbf{x} \sim p_I(\mathbf{x})} [\mathcal{L}_G^x([G \circ F](\mathbf{x}; \theta), \mathbf{x})] \\ &= \arg \min_{\theta} \int \mathcal{L}_G^x(\tilde{\mathbf{x}}, \mathbf{x}) p_I(\mathbf{x}) d\mathbf{x} \end{aligned} \quad (3)$$

where θ_g denotes the parameters of G , and $p_I(\mathbf{x})$ is the probability density function of \mathbf{x} . In particular, the generator G takes the deep feature in the deep representation space extracted by the network F as an input and produces the corresponding image in the image space where the reconstructed images $G(F(\mathbf{x}))$ are guarantee to be closed to its actual image \mathbf{x} measured by a distance metric \mathcal{L}_G^x .

Up to this point, there are two crucial problems related to the feature reconstruction problem, i.e. the design of the generator G and the choice of distance \mathcal{L}_G^x . In Section 3.2, we further discuss the design of our proposed generators. Then, we analyze the optional selection of \mathcal{L}_G^x followed by proposing a novel bijective metric.

3.2. The Proposed Network Architecture

As discussed in the previous section, the design of generator G plays an important role since it mainly affects to the reconstructed results. It is straightforward to adopt the common generator structure [39] for G where the generator takes the $F(\mathbf{x})$ as an input. However, the native structure design limits the generality of the generator G . In particular, the common design of G is a deterministic network where one input will produce only one image. In addition, along with the identity information, the input $F(\mathbf{x})$ may include other ‘‘background’’ information, e.g. pose, illuminations, expressions. Therefore, if we only take $F(\mathbf{x})$ as an input, it means that we implicitly enforces G to strictly model these factors. As a result, the reconstructed images will be not diversified and the training process of G will be less efficient.

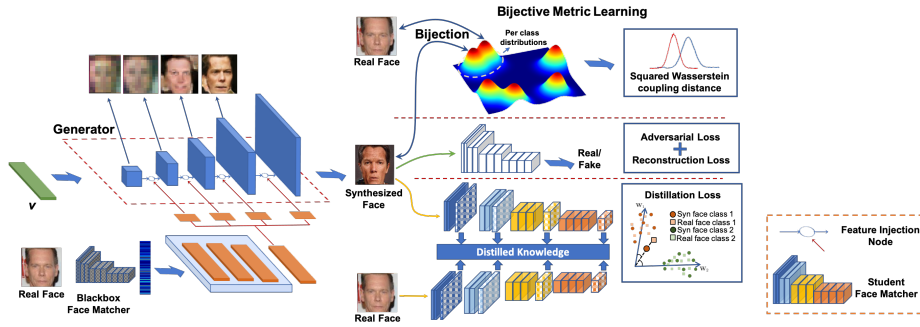


Figure 2: **The Proposed DAB-GAN Framework.** Given a high-level embedding representation, an *Attention-based Generator* injects that representation through-out its structure as the conditional information for all scales. The cost functions are designed with *Bijection Metric* to directly exploit ID distributions in image domain, and *Distillation Loss* to maximize the knowledge could be extracted from the blackbox matcher.

3.2.1. CNN-based Generator with Feature-Condition Structure

To address the aforementioned constrains, a novel feature-conditional structure is introduced as shown in Fig. 2. In this framework, a random variable \mathbf{v} is adopted as an additional input represented for the background factors. With our design, the vector \mathbf{v} will be a direct input of the generator and the information of deep feature $F(\mathbf{x})$ will be progressively injected through out the structure. By this design, the generator will gradually grow up the level of details of images and the feature $F(\mathbf{x})$ plays a role as the condition identity-related information for all reconstruction scales. Hence, the generator will give better synthetic results and the generality of the model is further enhanced. The detail of generator will be described in the experiments in Section 6.

Although CNN-based generator has achieved remarkable results in the image reconstruction tasks, this still suffer several issues. First, as the convolutional operators have local receptive field, the CNN-based generator are not able to model long-range dependencies. Although we could design a CNN network with a large number of convolutional layers, it is inefficient since it could lose the feature resolution and fine-grained features. Also, optimizing a huge CNN network is a difficult problem. Second, the spatial invariance property of the convolutional layers leave an issue on the adaptive ability of the generator to spatially varying and complex visual patterns. Moreover, even though we could design sophisticated CNN-based generators, training CNN-based generators within the GAN framework remains unstable and could result in mode collapse. Therefore, despite of the success of CNN-based generators, it is necessary to design a generator that can address the mentioned problems of CNN-based networks.

3.2.2. Attention-based Generator with Transformer

To address the problem of CNN-based generator, we introduce a novel attention-based generator. In particular, we design a convolution-free generator in which each block of the generator is purely designed by the Transformer block. The condition identity-related information, e.g $F(\mathbf{x})$, is progressively injected to all the network scale

through out the structure by the self-attention mechanism. With the design of Transformer, the generator can capture both local and global information by the attention mechanism. Also, the transformer-based generator is able to capture long-range dependencies without passing numerous layers as a CNN-based generator. As a result, the attention-based generator can model the complex visual structures. However, training a pure transformer-based generator is difficult since the vanilla Transformer network requires a large amount of memory when the image size scales up. To alleviate this issue, we adopt the memory-friendly transformer-based design of [33] to enhance the memory efficiency and maintain the synthesizing capability.

4. The Proposed Bijective Metric

4.1. The choices of \mathcal{L}_G^x and Their Limitations

The quality of reconstruction results is primarily dependent on the choice of \mathcal{L}_G^x . There are several prior works [40] have exploited different choices of \mathcal{L}_G^x to produce the good quality results. Overall, these choices could be divided into two groups: (1) *non-parametric*, and (2) *parametric* measurements.

Non-parametric metrics (i.e. direct metrics) such as ℓ_p or Total Variation typically measure the pixel-level difference between the reconstructed and ground-truth images. Although these metrics are straightforward to be adopted and optimized, they are *unstructured measurements* where a pixel is penalized independently to other pixels as well as the structured characteristics of the image. Moreover, they suffer other limitation in image quality. For example, images synthesized with ℓ_2 loss are surprisingly poor observed by humans [41].

Parametric metrics (i.e. indirect metrics or classifier-based metric) such as Adversarial loss or Perceptual Loss have proved their advantages in several tasks, e.g. Image Style Transfer [42], Image Synthesize [43]. A typical parametric metrics are computed via an additional mapping functions which are chosen according to the problem and the requirements of reconstruction quality. For example, the perceptual loss measures the differences between latent representations of images extracted via a classifier pre-trained on the ImageNet. Therefore, this metric is able to capture more semantic information such as differences of object structures in its measurement. On the other hand, Adversarial Loss learns a binary classifier (i.e. a discriminator) to penalizing the realism of the image. This type of metric, therefore, provides better reliable measurements in the terms of image realism and semantic information preservation in comparison to non-parametric metrics.

Although these parametric metrics have shown their advantages in several tasks, there are limitations when only the blackbox function F and its embedded features are given. In particular, as shown in prior adversarial attack studies [44, 45], as ***the function F is not an one-to-one mapping function from \mathcal{I} to \mathcal{F}*** , it is straightforward to find *two images sharing similar deep representations extracted by F that are drastically different in the image content*. As a result, without prior information about the subject identity of an image, reconstructing it from scratch may fail into the case where the reconstructed image \hat{I} is completely different from I but has similar deep feature representations. The current classifier-based metrics, e.g. adversarial training losses

or perceptual losses, are limited in maintaining the constraint “*the reconstructions of features of the same subject identity should be similar*”. This issue makes up the first criterion in our problem, i.e. **Identity Preservation**.

Additionally, learning with parametric metrics requires the gradients of the network structures during the optimization process. However, since the access to the network structure and intermediate features of the function F is unavailable due to the constraint of the blackbox setting, the function G is unable to directly exploit valuable information from the gradients of F and the intermediate representations. Therefore, the distance metrics defined via F , i.e. perceptual distance, is less effective compared to the whitebox setting. This points to the second criterion in our problem, i.e. **Blackbox Setting**.

To tackle these constraints, we propose a novel bijective metric to address these limitations for feature reconstruction task. Moreover, a distillation process is also proposed to exploit further information from the given blackbox recognition engine for reconstruction process.

4.2. The Proposed Bijective Metric

In this section, we initially present our proposed bijective metric for feature reconstruction that address the limitations of identity preservation. Next, we discuss the learning procedure of our proposed bijective metrics. Finally, we exploit the different aspects of the distillation approach to address the limitations of blackbox setting.

Many proposed metrics with sophisticated designs used for face recognition [46, 47, 48, 49, 50, 51] have been employed to improve the discriminative capability of features by maximizing intra-class compactness and inter-class separability with a large margin. Nevertheless, adopting these metrics for the feature reconstruction task is an infeasible solution since these metrics are limited as aforementioned in previous section (the problem of **Identity Preservation**).

Taking these limitations into consideration, we propose a bijective metric for the feature reconstruction task in which the mapping function from the image space to deep latent space is one-to-one. Thanks to bijective property, the distance between images will be equivalent to the distance between their deep latent features. As a result, the proposed metric is more aligned to the image domain and can be efficiently adopted for the reconstruction task. Also, as two different images cannot be mapped into the same latent features, the bijective metric is more reliable. It should be noticed that the direct access to $p_I(\mathbf{x})$ in Eqn. 3 is unavailable since we do not know the dataset set used to learn of the mapping function F . However, the approximation can be efficiently, practically adopted according to the prior knowledge about $p_I(\mathbf{x})$ that are facial images. Let $p_x(\mathbf{x})$ be a density function, an approximation of $p_I(\mathbf{x})$, estimated from an alternative large-scale face dataset. Therefore, the optimization of G in Eqn. (4), with an approximation $p_x(\mathbf{x})$ by drawing images from a large-scale face dataset, can be rewritten as:

$$\theta_g \approx \arg \min_{\theta} \int \mathcal{L}_G^x(\tilde{\mathbf{x}}, \mathbf{x}) p_x(\mathbf{x}) d\mathbf{x} \quad (4)$$

where $\tilde{\mathbf{x}} = [G \circ F](\mathbf{x}; \theta)$; Now, let $H : \mathcal{I} \mapsto \mathcal{Z}$ be a bijective function that map \mathbf{x} in the image space to a latent variable $\mathbf{z} = H(\mathbf{x})$ in the deep latent space. With to the

bijjective property, the optimization in Eqn. (4) is equivalent to.

$$\begin{aligned}
& \arg \min_{\theta} \int \mathcal{L}_G^z(H(\tilde{\mathbf{x}}), H(\mathbf{x})) p_x(\mathbf{x}) d\mathbf{x} \\
&= \arg \min_{\theta} \int \mathcal{L}_G^z(H(\tilde{\mathbf{x}}), H(\mathbf{x})) p_z(\mathbf{z}) |\det(\mathbf{J}_x^\top \mathbf{J}_x)|^{1/2} d\mathbf{z} \\
&= \arg \min_{\theta} \int \mathcal{L}_G^z(\tilde{\mathbf{z}}, \mathbf{z}) p_z(\mathbf{z}) |\det(\mathbf{J}_x^\top \mathbf{J}_x)|^{1/2} d\mathbf{z}
\end{aligned} \tag{5}$$

where $\tilde{\mathbf{z}} = H(\tilde{\mathbf{x}})$; $p_x(\mathbf{x}) = p_z(\mathbf{z}) |\det(\mathbf{J}_x^\top \mathbf{J}_x)|^{1/2}$ by the change of variable formula; \mathbf{J}_x is the Jacobian of H with respect to \mathbf{x} ; and \mathcal{L}_G^z is the distance metric in \mathcal{Z} . Intuitively, Eqn. (5) indicates that instead of computing the distance \mathcal{L}_G^x and estimating $p_x(\mathbf{x})$ directly in image domain, the optimization process can be equivalently accomplished via the distance \mathcal{L}_G^z and density $p_z(\mathbf{z})$ in \mathcal{Z} according to the bijjective property of H .

4.3. The Prior Distributions p_z .

In general, there are various choices for the prior distribution p_z and the ideal one should have two properties: (1) *simplicity in density estimation*, and (2) *easily sampling*. Motivated from these properties, Gaussian distribution has been chosen for p_z . It should be noticed that any other distribution types are still applicable in our framework if the chosen distribution satisfies the mentioned properties.

4.4. The Large-Margin Contrastive Distance Metric

Due to the choice of p_z as a Gaussian distribution, the distance between images in \mathcal{I} is equivalent to the deviation between Gaussians in the deep latent space. Therefore, we can effectively define \mathcal{L}_G^z as the squared Wasserstein coupling distance between two Gaussian distributions.

$$\begin{aligned}
\mathcal{L}_G^z(\tilde{\mathbf{z}}, \mathbf{z}) &= d(\tilde{\mathbf{z}}, \mathbf{z}) = \inf \mathbb{E}(\|\tilde{\mathbf{z}} - \mathbf{z}\|_2^2) \\
&= \|\tilde{\mu} - \mu\|_2^2 + \text{Tr}(\tilde{\Sigma} + \Sigma - 2(\tilde{\Sigma}^{1/2} \Sigma \tilde{\Sigma}^{1/2})^{1/2})
\end{aligned} \tag{6}$$

where $\{\tilde{\mu}, \tilde{\Sigma}\}$ and $\{\mu, \Sigma\}$ are the means and covariances of $\tilde{\mathbf{z}}$ and \mathbf{z} , respectively. The metric \mathcal{L}_G^z then can be further extended with image labels to improve the contrastive learning capability by reducing the distance between images of the same identity and enhance the margin between different identities.

$$\mathcal{L}_G^{z, id}(\tilde{\mathbf{z}}_1, \tilde{\mathbf{z}}_2) = \begin{cases} d(\tilde{\mathbf{z}}_1, \tilde{\mathbf{z}}_2) & \text{if } l_{\tilde{\mathbf{z}}_1} = l_{\tilde{\mathbf{z}}_2} \\ \max(0, d(\tilde{\mathbf{z}}_1, \tilde{\mathbf{z}}_2) - m) & \text{if } l_{\tilde{\mathbf{z}}_1} \neq l_{\tilde{\mathbf{z}}_2} \end{cases} \tag{7}$$

where m denotes hyper-parameter controlling the margin between classes; and $\{l_{\tilde{\mathbf{z}}_1}, l_{\tilde{\mathbf{z}}_2}\}$ denote the subject identity of $\{\tilde{\mathbf{z}}_1, \tilde{\mathbf{z}}_2\}$, respectively.

4.5. Learning the Bijection

To efficiently learn the bijjective mapping H , the multi-scale architecture network with tractable the log Jacobian determinant computation [52, 53] has been adopted as the backbone network. Additionally, to further improve the discriminative capability in the of H in the deep latent space \mathcal{Z} , the identity labels has been exploited during

the training process of H . In particular, given N classes of the training set, the Gaussian distributions with different means $\{\mu_i\}_{i=1}^N$ and covariances $\{\Sigma_i\}_{i=1}^N$ have been employed to enforce samples of each class distributed to its own prior distribution, i.e. $\mathbf{z}_k \sim \mathcal{N}(\mu_k, \Sigma_k)$. Formally, the mapping H can be learned by the negative log-likelihood loss formulated as follows:

$$\begin{aligned} \theta_H^* &= -\arg \min_{\theta_H} \mathbb{E}_{\mathbf{x} \sim p_x(\mathbf{x})} \log p_x(\mathbf{x}, k; \theta_H) \\ &= -\arg \min_{\theta_H} \mathbb{E}_{\mathbf{x} \sim p_x(\mathbf{x})} \left[\log p_z(\mathbf{z}, k; \theta_H) + \frac{1}{2} \log |\det(\mathbf{J}_{\mathbf{x}}^\top \mathbf{J}_{\mathbf{x}})| \right] \end{aligned} \quad (8)$$

4.5.1. Structuring of Bijection Latent Space with ID labels

Different from previous works where only an Gaussian distribution, i.e. Normal Distribution, is designed for the Bijection’s Latent space, multiple Gaussians are required to form the Latent space where images of each subject ID/class distribute within a Gaussian distribution in that latent space. In order to improve the discriminative property of H in latent space \mathcal{Z} , we propose to exploit the ID label in training process of H . Particularly, the means and covariances of Gaussian distributions are pre-defined for all C classes:

$$\begin{aligned} \boldsymbol{\mu}_c &= \mathbf{1}c; \boldsymbol{\Sigma} = \mathbf{I} \\ \mathbf{z}_c &\sim \mathcal{N}(\boldsymbol{\mu}_c, \mathbf{I}) \end{aligned} \quad (9)$$

where $\mathbf{1}$ is the all-one vector, the subscript c denotes for class c .

4.6. Learning from Distillation Knowledge

In the traditional approach, the generator G can be still learned by adopting the perceptual distance [54] to compute the difference between deep feature representations, i.e. $F(\tilde{\mathbf{I}})$ and $F(\mathbf{I})$. However, as aforementioned in Section 4.1, the direct access to the network F , i.e. the gradients and the intermediate representations, is unavailable due to the blackbox setting. To maximize the information that can be exploited from the recognition engine F , we propose to distill the matching knowledge from the blackbox F to a “student“ function F^S . Then, distilled knowledge adapted to F^S will be employed to train the generator G . There are two important purposes shown from the distillation process. First, the student network F^S can mimic the behavior of the network F by aligning its deep feature space to the one produced by F and maintaining the semantic information of extracted features the reconstruction process. Second, with our designed F^S , the knowledge about the embedding process of F , i.e. the network gradients and intermediate representations, will become transparent. Therefore, knowledge from the blackbox function F can be maximally exploited via the student function F^S .

Mathematically, let $F^S : \mathcal{I} \mapsto \mathcal{F}$ and $F^S = F_1^S \circ F_2^S \dots \circ F_n^S$ be the composition of n -sub components. The knowledge from F can be distilled to F^S by aligning their extracted features defined as follows:

$$\begin{aligned} \theta_S &= \arg \min_{\theta_S} \mathcal{L}_S = \mathbb{E}_{\mathbf{x} \sim p_x} d_{\text{distill}}(F(\mathbf{x}), F_S(\mathbf{x}; \theta_S)) \\ &= \arg \min_{\theta_S} \mathbb{E}_{\mathbf{x} \sim p_x} \left\| 1 - \frac{F(\mathbf{x})}{\|F(\mathbf{x})\|} * \frac{F^S(\mathbf{x}; \theta_S)}{\|F^S(\mathbf{x}; \theta_S)\|} \right\|_2^2 \end{aligned} \quad (10)$$

Hence, the generator G can be further enhanced via the distilled knowledge of not only final embedding features but also the intermediate representations via the student function F^S formed as follows:

$$\begin{aligned} \mathcal{L}_G^{distill}(\tilde{\mathbf{x}}, \mathbf{x}) &= \sum_{j=1}^n \lambda_j \frac{\|F_j^S(\tilde{\mathbf{x}}; \theta_S) - F_j^S(\mathbf{x}; \theta_S)\|}{W_j H_j C_j} \\ &+ \lambda_a \left\| 1 - \frac{F^S(\tilde{\mathbf{x}}; \theta_S)}{\|F^S(\tilde{\mathbf{x}}; \theta_S)\|} * \frac{F^S(\mathbf{x}; \theta_S)}{\|F^S(\mathbf{x}; \theta_S)\|} \right\|_2^2 \end{aligned} \quad (11)$$

where $\{\lambda_j\}_1^n$ and λ_a denote the hyper-parameters controlling the impacts of two terms. The first term of $\mathcal{L}_G^{distill}(\tilde{\mathbf{x}}, \mathbf{x})$ aims to penalize the differences between the intermediate structure of the desired and reconstructed facial images while the second term validates the similarity of their final deep features.

5. Attention-based Bijective Generative Adversarial Networks

In this section, we will present the training procedure of our proposed network. Figure 2 illustrates the proposed framework with Bijective Metric and Distillation Process mentioned in the previous sections to train the generator G .

5.1. Training Procedure

Given the input image \mathbf{x} , the generator G takes the deep feature $F(\mathbf{x})$ as the input and aims to reconstruct the image $\tilde{\mathbf{x}}$ so that the reconstructed image $\tilde{\mathbf{x}}$ is as similar to the original image \mathbf{x} as possible in terms of identity and visual appearance. The GAN-based generator architecture [55] is adopted for our generator structure G . The entire framework is optimized by using different criteria defined as follows.

$$\begin{aligned} \mathcal{L}_G &= \lambda_b \mathcal{L}^{biject} + \lambda_d \mathcal{L}^{distill} + \lambda_{adv} \mathcal{L}^{adv} + \lambda_r \mathcal{L}^{recon} \\ \mathcal{L}^{biject} &= \mathbb{E}_{\mathbf{x} \sim p_x} [\mathcal{L}_G^x((G \circ F)(\mathbf{x}; \theta), \mathbf{x})] \\ &+ \mathbb{E}_{\mathbf{x}_1, \mathbf{x}_2 \sim p_x} [\mathcal{L}_G^{x_{id}}((G \circ F)(\mathbf{x}_1; \theta), (G \circ F)(\mathbf{x}_2; \theta))] \\ &= \mathbb{E}_{\mathbf{z} \sim p_z} [\mathcal{L}_G^z(\tilde{\mathbf{z}}, \mathbf{z})] + \mathbb{E}_{\mathbf{z}_1, \mathbf{z}_2 \sim p_z} [\mathcal{L}_G^{z_{id}}(\tilde{\mathbf{z}}_1, \tilde{\mathbf{z}}_2)] \\ \mathcal{L}^{distill} &= \mathbb{E}_{\mathbf{x} \sim p_x} [\mathcal{L}_G^{distill}((G \circ F)(\mathbf{x}; \theta), \mathbf{x})] \\ \mathcal{L}^{adv} &= \mathbb{E}_{\mathbf{x} \sim p_x} [D((G \circ F)(\mathbf{x}; \theta))] \\ \mathcal{L}^{recon} &= \mathbb{E}_{\mathbf{x} \sim p_x} [\| (G \circ F)(\mathbf{x}) - \mathbf{x} \|_1] \end{aligned} \quad (12)$$

where $\{\mathcal{L}^{biject}, \mathcal{L}^{distill}, \mathcal{L}^{adv}, \mathcal{L}^{recon}\}$ denote the bijective, distillation, adversarial, and reconstruction losses, respectively. D is a discriminator distinguishing the real images from a synthesized one. $\{\lambda_b, \lambda_d, \lambda_{adv}, \lambda_r\}$ are their parameters controlling their relative importance. The bijective metric \mathcal{L}^{biject} and the distillation loss $\mathcal{L}^{distill}$ constrain the identity preservation. The reconstruction loss \mathcal{L}^{recon} enforces the similarity between the original image and the reconstructed image; meanwhile, via the discriminator D , the adversarial loss \mathcal{L}^{adv} penalizes the realism of the synthesized image. The discriminator D is alternately updated along with the generator G as follows.

$$\begin{aligned} \mathcal{L}_D &= \mathbb{E}_{\mathbf{x} \sim p_x} [D((G \circ F)(\mathbf{x}; \theta))] - \mathbb{E}_{\mathbf{x} \sim p_x} [D(\mathbf{x})] \\ &+ \lambda \mathbb{E}_{\tilde{\mathbf{x}} \sim p_{\tilde{\mathbf{x}}}} [(\|\nabla_{\tilde{\mathbf{x}}} D(\tilde{\mathbf{x}})\|_2 - 1)^2] \end{aligned} \quad (13)$$

where $p_{\hat{x}}$ is the random interpolation distribution between real and generated images [56]. Finally, the GAN-based minimax strategy is adopted to train the entire framework.

5.2. Exponential Weighting Decay

As the progressive growing training manner [39] starts learning from the low resolution and gradually increasing the level of details, it is efficient for learning the images in general. Nevertheless, the strategy is inefficient in the term of maintaining the identity information. Particularly, in the initial scales at the low resolutions where the face images are still blurry, it is difficult to control the subject identity of faces to be synthesized. Meanwhile, in the later scales when the generator becomes more mature and learns to add more details, the identities of those faces have already been structured and become hard to change. There is a trade-off between realism and identity preservation during the progressive training process. Therefore, we propose an exponential weighting scheme for emphasizing on the identity preservation in the early stages and penalizing the realism in the later stages. Formally, the hyper-parameter set $\{\lambda_b, \lambda_d, \lambda_{adv}, \lambda_r\}$ is progressively defined as follows:

$$\begin{aligned}
 \lambda_b &= \alpha e^{R_M - R(i)} \\
 \lambda_d &= e^{R_M - R(i)} \\
 \lambda_{adv} &= \beta e^{R(i)} \\
 \lambda_r &= e^{R_M - R(i)}
 \end{aligned} \tag{14}$$

where $R(i)$ denotes the current scales of stage i and R_M is the maximum scales to be learned by G .

6. Experiments

6.1. Datasets and Model Configurations

6.1.1. Dataset

The training dataset includes the publicly available Casia-WebFace [57] consisting of 490K labeled facial images of over 10K subjects. Since we focus on the open-set scenario, the duplicated subjects between training and testing sets are removed to ensure no overlapping between them. For validation, as common practices of the attribute learning and image quality evaluation, we adopt the testing split of 10K images from CelebA [58] to validate the reconstruction quality. For ID preservation, we explore LFW [59], AgeDB [60], and CFP-FP [61] which provide the standard face verification protocols against different in-the-wild face variations. Since each face matcher engine requires different preprocessing process, the training and testing data are aligned to the required template accordingly.

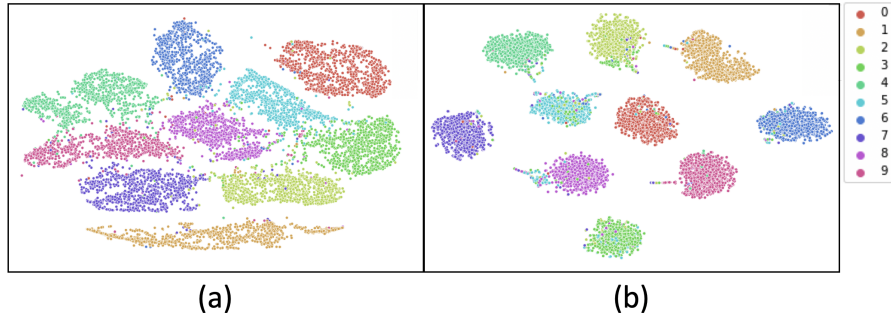


Figure 3: **The distributions of synthesized MNIST samples** on testing set (a) without, and (b) with adopting Bijective Metric.

6.1.2. Model Configurations

Network Architectures. For our CNN-based generator, the generator structure from PO-GAN [39] is utilized which consists of 5 convolutional blocks for G whereas the feature conditional branch has 8 fully connected layers. The combination of five consecutive blocks of 2 convolution and 1 downsampling operators is included in the discriminator D . The adoption of minibatch-stdev operator continued by convolution and fully connected is done in the last block of D . The application of AdaIN operator [62] is done for feature injection node. A configuration is setup for the bijection H , which has 5 sub-mapping functions where each of them is represented as two 32-feature-map residual blocks. The training of this structure is done using log-likelihood objective function on Casia-WebFace. Resnet-50 [29] is adopted for F^S .

Meanwhile, the structure from TransGAN [33] is adopted for our attention-based generator. Particularly, the attention-based transformer has 5 blocks of Transformer. Instead of using the vanilla self-attention layer in each block of transformer, the grid self-attention is utilized to reduce the memory bottleneck when the resolution is scaling up to high resolution. The multi-scale discriminator from [33] is adopted for our discriminator D . In our paper, we denotes the CNN-based generator and attention-based generator as DiBiGAN and DAB-GAN, respectively.

Optimization Configurations. The entire framework is implemented in Tensorflow and all the models are trained on a machine with four GPUs of NVIDIA RTX Quadro P8000. The batch size is set based on the resolution of output images, for the very first resolution of output images (4×4), the batch size is set to 128, the batch size will be divided by two when the resolution of images is doubled. The Adam Optimizer with the started learning rate of 0.0015 has been employed to to optimize the network. We empirically set $\{\alpha = 0.001, \beta = 1.0, \lambda_j = 1, \lambda_a = 10.0\}$ to maintain the balanced values between loss terms.

6.2. Ablation Study

To illustrate the effectiveness of our proposed bijective metric for the feature reconstruction task, we conduct an ablative experiment on MNIST [63] with LeNet [64] as the function F . To remove the effects of other factor, we consider the whitebox

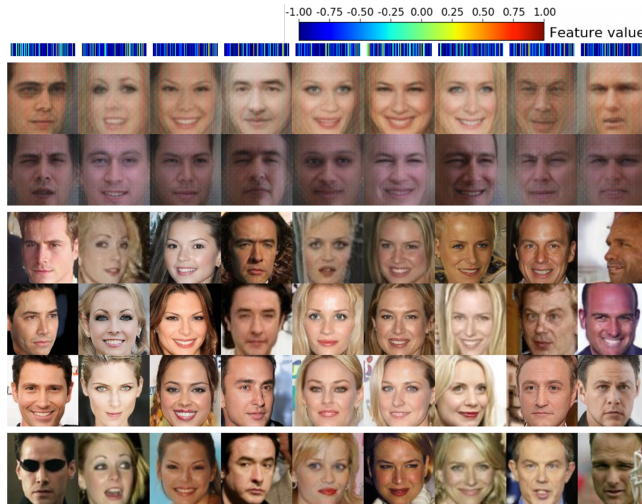


Figure 4: **Feature Reconstruction against in-the-wild facial variations.** For each subject, given an input feature (1st row), while VGG-NBNet [14] and MPIE-NBNet [14] (2nd and 3rd rows) reconstruct faces with limited quality, DiBiGAN in whitebox mode (4th row), DiBiGAN in blackbox mode (5th row), and DABGAN in blackbox mode (6th row) are able to produce realistic faces with better ID preservation comparable to real faces (6th row).

mode in this experiment where F is directly used in $\mathcal{L}^{distill}$. The entire training set of MNIST and their their 1×1024 feature vectors are used to train the generator G . Since the image size of MNIST is 32×32 , we only use three convolution blocks for our CNN-based generator and discriminator. The resulting distributions of synthetic testing images of all classes without and with our proposed bijective metric \mathcal{L}^{biject} are illustrated in Fig. 3. As shown in this figure, the distribution with our bijective metric learning (Fig. 3(b)) is supervised with more direct metric learning mechanism in image domain, and, therefore, shows the advantages with enhanced intra-class and inter-class distributions compared to the case where the generator G is learned with only classifier-based metrics (Fig. 3(a)).

6.3. Face Reconstruction Results

6.3.1. Reconstruction Result with Features of Frontal Face

With our proposed method, given only the deep features extracted from F on testing images, the generator G is able to reconstruct the subjects' faces. Fig. 4 illustrate the qualitative comparison of our synthetic faces with other baselines. In particular, our generator G is able to reconstruct realistic faces even when their embedding features are extracted from faces with a wide range of in-the-wild variations. Importantly, our proposed method successfully preserves the ID features of these subjects in both white-box and blackbox settings. In the whitebox setting, since the structure of F is accessible, the learning process can effectively exploit different aspects of embedding process from F and produce a generator G that depicts better facial features of the real faces. Meanwhile, although the accessible information is very limited in blackbox setting, the

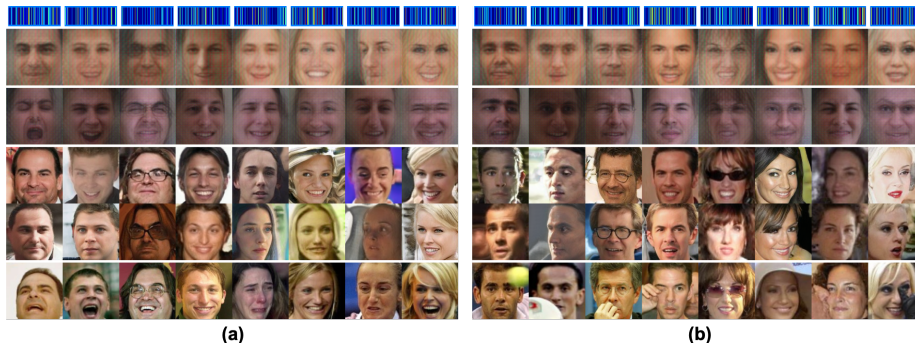


Figure 5: **Feature Reconstruction against expressions (a) and occlusions (b)**. For each subject, the 1st row shows the input feature. The next five rows are VGG-NBNet [14], MPIE-NBNet [14], Our DibiGAN in whitebox and blackbox settings, and Real Faces, respectively.

learned generator G is still able to observe the distill knowledge of F^S and efficiently fill the knowledge gap with whitebox setting. As shown in Fig. 4, we achieve better face in terms of image quality and ID preservation compared to NBNet [14]. Moreover, the quality of synthetic faces reconstructed by attention-based generator is better than the ones synthesized by the CNN-based generator.

6.3.2. Effectiveness of Occlusions and Expressions

Fig. 5 demonstrates our synthesis based on attributes of faces with both expressions and occlusions. Similarly to the previous experiment, our model portrays realistic faces with comparable ID features as in real faces. The quality of the reconstructed faces consistently outperform NBNet in both realistic and ID categories. The success of robustly dealing with those challenging factors can be attributed to two factors: (1) the matcher F was trained to ignore those facial variations in its embedding features; and (2) both bijective metric learning and distillation processes can efficiently exploit necessary knowledge from F as well as real face distributions in image domain for the synthesis process.

6.3.3. Effectiveness of Background Information

As mentioned in Sec. 3.2.1, the variable \mathbf{v} is utilized to represent background factors, allowing G to focus on modeling ID characteristics. As a result, multiple situations of that face may be synthesized by fixing the input feature and modifying the variable values, as illustrated in Fig. 6. These findings highlight the benefits of our model structure in terms of its capacity to capture numerous aspects for the reconstruction process.

6.3.4. Effectiveness of Different Features of Same Subject

Fig. 7 demonstrates the benefits of our technique for synthesizing faces from diverse feature representations of the same subject. These findings highlight the benefits of the proposed bijective metric in improving the border between classes and constraining the similarity of reconstructed faces of the same subject in the image domain. As a

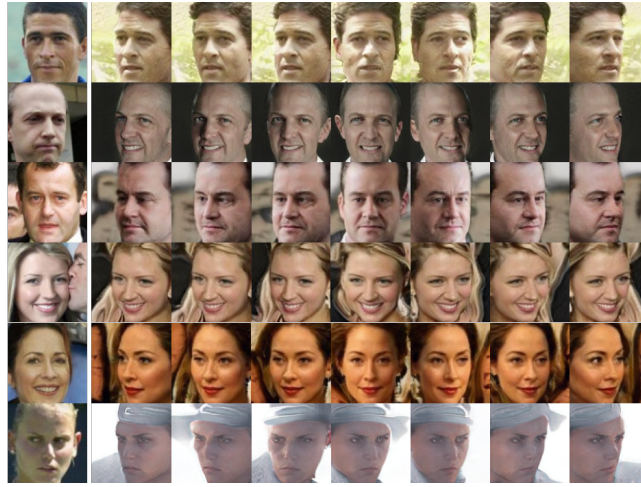


Figure 6: From the input features, our model can synthesize various conditions of a face by varying the “background” variable v .

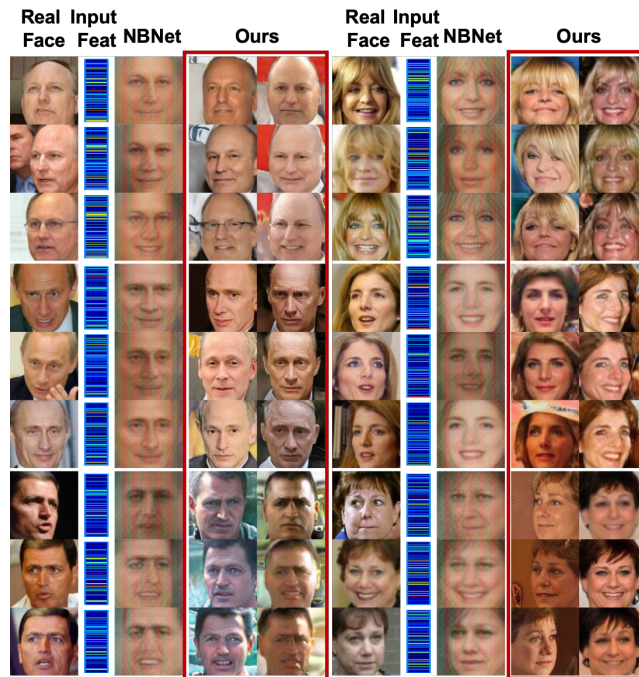


Figure 7: **Feature Reconstruction against features of the same subject.** For each subject, the first and second columns show different real faces and their features of a subject. Compared to VGG-NBNet [14] (third column), our DibiGAN in whitebox and blackbox modes can effectively preserve the ID of the subjects.

Table 2: **Realism Quality and Matching Accuracy.** Comparison results in Multi-Scale Structural Similarity (MS-SSIM) (*the smaller value is better*); Inception score and Matching Accuracy (*the higher value is better*). For each configuration in (A)-(C), (D)-(F), and (G)-(I), each loss function is cumulative enable on the top of the previous configuration. — denotes “not applicable”.

	White-box Reconstruction					Black-box Reconstruction				
	CelebA		LFW	AgeDB	CFP-FP	CelebA		LFW	AgeDB	CFP-FP
MS-SSIM	IS	MS-SSIM				IS				
Real Faces ¹	0.305	3.008	99.78%	98.40%	97.10%	0.305	3.008	99.70%	96.80%	93.10%
VGG-NBNet [14]	—	—	—	—	—	0.661	1.387	91.42%	80.42%	74.63%
MPIE-NBNet [14]	—	—	—	—	—	0.592	1.484	93.17%	79.45%	78.51%
(A) PO_GAN [39]	0.331	2.226	68.20%	63.42%	68.89%	0.315	2.227	66.63%	62.37%	65.59%
(B) + $\mathcal{L}^{distill}$	0.343	2.073	96.03%	83.33%	79.07%	0.337	2.238	94.95%	81.56%	78.80%
(C) + \mathcal{L}^{bijeet}	0.358	2.052	98.10%	88.16%	88.01%	0.360	2.176	97.30%	85.71%	82.51%
(D) DiBiGAN	0.316	2.343	79.82%	77.20%	81.71%	0.305	2.463	77.57%	76.83%	80.66%
(E) + $\mathcal{L}^{distill}$	0.306	2.349	97.76%	86.61%	89.20%	0.305	2.423	97.06%	91.70%	84.83%
(F) + \mathcal{L}^{bijeet}	0.310	2.531	99.18%	94.18%	92.67%	0.303	2.422	99.13%	93.53%	89.03%
(G) DAB-GAN	0.315	2.361	82.41%	80.12%	82.62%	0.321	2.425	79.28%	78.72%	81.85%
(H) + $\mathcal{L}^{distill}$	0.302	2.425	99.02%	92.25%	92.17%	0.318	2.442	98.96%	92.35%	86.72%
(I) + \mathcal{L}^{bijeet}	0.319	2.367	99.52%	95.58%	93.11%	0.301	2.322	99.21%	94.18%	92.17%

consequence, reconstructed faces from the same subject ID not only retain the features of that subject (i.e., are comparable to actual faces), but also share similar features.

6.3.5. Face Verification Results

In order to quantitatively evaluate the realism of our synthetic faces and how well the proposed approach can preserve the ID feature, three metrics are adopted: (1) Face verification accuracy; (2) Multi-scale Structural similarity (MS-SSIM) [65]; (3) Inception Score (IS) [66];

ID Preservation. Our model is tested against LFW, AgeDB, and CFP-FP, with an image in each positive pair replaced by the reconstructed one and the remaining image of that pair preserved as the reference actual face. Table 2 reports the matching accuracy. Each component in our framework highlights the advantages and contributions through these results. In comparison to the PO_GAN structure, our Feature-Conditional Structure (DiBiGAN) allows for greater flexibility in modeling ID characteristics and achieves higher matching accuracy. In conjunction with distilled information from F^S , the Generator delivers a significant increase in accuracy, closing the gap to actual faces to only 2.02% and 2.722% on LFW in whitebox and blackbox settings, respectively. By including the bijective measure, these gaps are decreased to 0.6% and 0.65% for the two settings, respectively. Moreover, with the attention-based generator (DAB-GAN), we further improve the verification performance and reduce the gap between synthetic faces and real faces in both whitebox and blackbox settings.

Reconstructions against different Face Recognition Engines. To demonstrate the effectiveness of our proposed approach, we tested it against several face recognition engines, as shown in Table 3. All generators are set to blackbox mode, which means that only the final extracted features are available. Our reconstructed faces can retain the ID information and attain the same level of accuracy as actual faces. These results highlight our model’s effectiveness in capturing the behaviors of the feature extraction functions F and providing high-quality reconstructions and maintaining the verification performance.

Table 3: Accuracy against different blackbox face matchers.

Matcher	Approach	LFW	AgeDB	CFP-FP
ArcFace[46]	Real	99.78%	98.40%	97.1%
	DiBiGAN	99.13%	93.53%	89.03%
	DAB-GAN	99.21%	94.18%	92.17%
FaceNet[18]	Real	99.55%	90.16%	94.05%
	DiBiGAN	98.05%	89.80%	87.19%
	DAB-GAN	98.25%	89.80%	88.51%
SphereFacePlus[47]	Real	98.92%	91.92%	91.16%
	DiBiGAN	97.21%	88.98%	86.86%
	DAB-GAN	97.95%	89.12%	87.75%

6.3.6. Face Quality Results

To evaluate the realism of the synthetic faces, we synthesize all faces of CelebA testing set in several training configurations as shown in Table 2 where each loss function in cumulatively enables on the top of the previous configuration. As the baseline protocol [39], we compared MS-SSIM and IS metrics between our synthetic faces and other baselines (PO_GAN [39] and NBNNet [14]) in both whitebox and blackbox settings. It should be noted that the adversarial and reconstruction losses for configs (A), (D), and (G). For all configs (A), (B), and (C), the PO_GAN baseline takes only the embedding features as its input. As shown in Table 2, the qualitative results have shown that our approach maintains the competitive reconstruction quality as PO_GAN and having a small gap between our synthetic faces and real faces. Moreover, our synthetic images consistently outperforms NBNNet in both MS-SSIM and IS metrics.

7. Conclusions

This work has introduced a novel attention-based structure with Bijective Metric Learning for feature reconstruction problem to reconstruct the subjects’ faces given their deep blackboxed features. The feature reconstruction problem is considered in the context of blackbox setting and open-set problem which make the problem becoming challenging. Thanks to the proposed Bijective Metric, the presented attention-based generator, and the Distillation Knowledge, our DAB-GAN effectively maximizes the information to be exploited from a given blackbox face recognition engine. The intensive experiments on a wide range of in-the-wild face variations against different face matching engines have demonstrated the advantages of our method on synthesizing realistic faces with subject’s identity preservation.

References

- [1] W. Zhao, R. Chellappa, P. J. Phillips, A. Rosenfeld, Face recognition: A literature survey, *ACM computing surveys (CSUR)* 35 (4) (2003) 399–458.
- [2] A. Ilyas, L. Engstrom, A. Athalye, J. Lin, Black-box adversarial attacks with limited queries and information, in: J. Dy, A. Krause (Eds.), *Proceedings of the 35th*

- International Conference on Machine Learning, Vol. 80 of Proceedings of Machine Learning Research, PMLR, Stockholmsmässan, Stockholm Sweden, 2018, pp. 2137–2146.
URL <http://proceedings.mlr.press/v80/ilyas18a.html>
- [3] A. Ilyas, L. Engstrom, A. Madry, Prior convictions: Black-box adversarial attacks with bandits and priors, in: International Conference on Learning Representations, 2019.
URL <https://openreview.net/forum?id=BkMiWhR5K7>
- [4] S. Thys, W. Van Ranst, T. Goedeme, Fooling automated surveillance cameras: Adversarial patches to attack person detection, in: The IEEE Conference on Computer Vision and Pattern Recognition (CVPR) Workshops, 2019.
- [5] K. Bousmalis, N. Silberman, D. Dohan, D. Erhan, D. Krishnan, Unsupervised pixel-level domain adaptation with generative adversarial networks, in: Proceedings of the IEEE conference on computer vision and pattern recognition, 2017, pp. 3722–3731.
- [6] E. Tzeng, J. Hoffman, K. Saenko, T. Darrell, Adversarial discriminative domain adaptation, in: Proceedings of the IEEE conference on computer vision and pattern recognition, 2017, pp. 7167–7176.
- [7] A. Athalye, L. Engstrom, A. Ilyas, K. Kwok, Synthesizing robust adversarial examples, in: J. Dy, A. Krause (Eds.), Proceedings of the 35th International Conference on Machine Learning, Vol. 80 of Proceedings of Machine Learning Research, PMLR, Stockholmsmässan, Stockholm Sweden, 2018, pp. 284–293.
- [8] F. Cole, D. Belanger, D. Krishnan, A. Sarna, I. Mosseri, W. T. Freeman, Synthesizing normalized faces from facial identity features, in: The IEEE Conference on Computer Vision and Pattern Recognition (CVPR), 2017.
- [9] A. Dosovitskiy, T. Brox, Inverting visual representations with convolutional networks, in: The IEEE Conference on Computer Vision and Pattern Recognition (CVPR), 2016.
- [10] Y. Song, R. Shu, N. Kushman, S. Ermon, Constructing unrestricted adversarial examples with generative models, in: S. Bengio, H. Wallach, H. Larochelle, K. Grauman, N. Cesa-Bianchi, R. Garnett (Eds.), Advances in Neural Information Processing Systems 31, Curran Associates, Inc., 2018, pp. 8312–8323.
- [11] A. Zhmoginov, M. Sandler, Inverting face embeddings with convolutional neural networks, ArXiv abs/1606.04189.
- [12] Y. Zhang, R. Jia, H. Pei, W. Wang, B. Li, D. Song, The secret revealer: Generative model-inversion attacks against deep neural networks, in: Proceedings of the IEEE/CVF Conference on Computer Vision and Pattern Recognition, 2020, pp. 253–261.

- [13] A. Razzhigaev, K. Kireev, E. Kaziakhmedov, N. Tursynbek, A. Petiushko, Black-box face recovery from identity features, in: European Conference on Computer Vision, Springer, 2020, pp. 462–475.
- [14] G. Mai, K. Cao, P. C. Yuen, A. K. Jain, On the reconstruction of face images from deep face templates, IEEE transactions on pattern analysis and machine intelligence 41 (5) (2018) 1188–1202.
- [15] A. Mahendran, A. Vedaldi, Understanding deep image representations by inverting them., in: CVPR, IEEE Computer Society, 2015, pp. 5188–5196.
- [16] C. N. Duong, T.-D. Truong, K. Luu, K. G. Quach, H. Bui, K. Roy, Vec2face: Unveil human faces from their blackbox features in face recognition, in: Proceedings of the IEEE/CVF Conference on Computer Vision and Pattern Recognition, 2020, pp. 6132–6141.
- [17] J. Yosinski, J. Clune, A. Nguyen, T. Fuchs, H. Lipson, Understanding neural networks through deep visualization, arXiv preprint arXiv:1506.06579.
- [18] F. Schroff, D. Kalenichenko, J. Philbin, Facenet: A unified embedding for face recognition and clustering, in: Proceedings of the IEEE conference on computer vision and pattern recognition, 2015, pp. 815–823.
- [19] Z. Yang, J. Zhang, E.-C. Chang, Z. Liang, Neural network inversion in adversarial setting via background knowledge alignment, in: Proceedings of the 2019 ACM SIGSAC Conference on Computer and Communications Security, CCS '19, ACM, New York, NY, USA, 2019, pp. 225–240. doi:10.1145/3319535.3354261.
URL <http://doi.acm.org/10.1145/3319535.3354261>
- [20] J. Johnson, A. Alahi, L. Fei-Fei, Perceptual losses for real-time style transfer and super-resolution, in: European conference on computer vision, Springer, 2016, pp. 694–711.
- [21] T. Brunner, F. Diehl, A. Knoll, Copy and paste: A simple but effective initialization method for black-box adversarial attacks, ArXiv abs/1906.06086.
- [22] S. Cheng, Y. Dong, T. Pang, H. Su, J. Zhu, Improving black-box adversarial attacks with a transfer-based prior, ArXiv abs/1906.06919.
- [23] Y. Liu, X. Chen, C. Liu, D. X. Song, Delving into transferable adversarial examples and black-box attacks, ArXiv abs/1611.02770.
- [24] S.-M. Moosavi-Dezfooli, A. Fawzi, P. Frossard, Deepfool: A simple and accurate method to fool deep neural networks, 2016 IEEE Conference on Computer Vision and Pattern Recognition (CVPR) (2015) 2574–2582.
- [25] S. N. Shukla, A. K. Sahu, D. Willmott, J. Z. Kolter, Black-box adversarial attacks with bayesian optimization, ArXiv abs/1909.13857.

- [26] A. Vaswani, N. Shazeer, N. Parmar, J. Uszkoreit, L. Jones, A. N. Gomez, Ł. Kaiser, I. Polosukhin, Attention is all you need, in: *Advances in neural information processing systems*, 2017, pp. 5998–6008.
- [27] J. Devlin, M.-W. Chang, K. Lee, K. Toutanova, Bert: Pre-training of deep bidirectional transformers for language understanding, *arXiv preprint arXiv:1810.04805*.
- [28] T. B. Brown, B. Mann, N. Ryder, M. Subbiah, J. Kaplan, P. Dhariwal, A. Neelakantan, P. Shyam, G. Sastry, A. Askell, et al., Language models are few-shot learners, *arXiv preprint arXiv:2005.14165*.
- [29] K. He, X. Zhang, S. Ren, J. Sun, Deep residual learning for image recognition, in: *Proceedings of the IEEE conference on computer vision and pattern recognition*, 2016, pp. 770–778.
- [30] S. Ren, K. He, R. Girshick, J. Sun, Faster r-cnn: Towards real-time object detection with region proposal networks, *Advances in neural information processing systems* 28 (2015) 91–99.
- [31] X. Zhu, W. Su, L. Lu, B. Li, X. Wang, J. Dai, Deformable detr: Deformable transformers for end-to-end object detection, *arXiv preprint arXiv:2010.04159*.
- [32] N. Carion, F. Massa, G. Synnaeve, N. Usunier, A. Kirillov, S. Zagoruyko, End-to-end object detection with transformers, in: *European Conference on Computer Vision*, Springer, 2020, pp. 213–229.
- [33] Y. Jiang, S. Chang, Z. Wang, Transgan: Two pure transformers can make one strong gan, and that can scale up, *Advances in Neural Information Processing Systems* 34.
- [34] C.-H. Lin, E. Yumer, O. Wang, E. Shechtman, S. Lucey, St-gan: Spatial transformer generative adversarial networks for image compositing, in: *Proceedings of the IEEE Conference on Computer Vision and Pattern Recognition*, 2018, pp. 9455–9464.
- [35] D. A. Hudson, C. L. Zitnick, Generative adversarial transformers, *arXiv preprint arXiv:2103.01209*.
- [36] P. Esser, R. Rombach, B. Ommer, Taming transformers for high-resolution image synthesis, in: *Proceedings of the IEEE/CVF Conference on Computer Vision and Pattern Recognition*, 2021, pp. 12873–12883.
- [37] M. Chen, A. Radford, R. Child, J. Wu, H. Jun, D. Luan, I. Sutskever, Generative pretraining from pixels, in: *International Conference on Machine Learning*, PMLR, 2020, pp. 1691–1703.
- [38] P. Upchurch, J. Gardner, G. Pleiss, R. Pless, N. Snavely, K. Bala, K. Q. Weinberger, Deep feature interpolation for image content changes, in: *The IEEE Conference on Computer Vision and Pattern Recognition (CVPR)*, 2017.

- [39] T. Karras, T. Aila, S. Laine, J. Lehtinen, Progressive growing of gans for improved quality, stability, and variation, arXiv preprint arXiv:1710.10196.
- [40] J. Smith, S. Schaefer, Bijective parameterization with free boundaries, *ACM Transactions on Graphics (TOG)* 34 (4) (2015) 1–9.
- [41] L. Zhang, L. Zhang, X. Mou, D. Zhang, A comprehensive evaluation of full reference image quality assessment algorithms, in: *2012 19th IEEE International Conference on Image Processing*, 2012, pp. 1477–1480. doi:10.1109/ICIP.2012.6467150.
- [42] L. A. Gatys, A. S. Ecker, M. Bethge, Image style transfer using convolutional neural networks, in: *Proceedings of the IEEE conference on computer vision and pattern recognition*, 2016, pp. 2414–2423.
- [43] S. Reed, Z. Akata, X. Yan, L. Logeswaran, B. Schiele, H. Lee, Generative adversarial text to image synthesis, in: *International Conference on Machine Learning*, PMLR, 2016, pp. 1060–1069.
- [44] L. Engstrom, A. Ilyas, S. Santurkar, D. Tsipras, B. Tran, A. Madry, Learning perceptually-aligned representations via adversarial robustness, arXiv preprint arXiv:1906.00945.
- [45] S. Santurkar, D. Tsipras, B. Tran, A. Ilyas, L. Engstrom, A. Madry, Computer vision with a single (robust) classifier, in: *ArXiv preprint arXiv:1906.09453*, 2019.
- [46] J. Deng, J. Guo, N. Xue, S. Zafeiriou, Arcface: Additive angular margin loss for deep face recognition, in: *Proceedings of the IEEE Conference on Computer Vision and Pattern Recognition*, 2019, pp. 4690–4699.
- [47] W. Liu, R. Lin, Z. Liu, L. Liu, Z. Yu, B. Dai, L. Song, Learning towards minimum hyperspherical energy, in: *NIPS*, 2018.
- [48] W. Liu, Y. Wen, Z. Yu, M. Li, B. Raj, L. Song, Sphereface: Deep hypersphere embedding for face recognition, in: *Proceedings of the IEEE conference on computer vision and pattern recognition*, 2017, pp. 212–220.
- [49] H. Wang, Y. Wang, Z. Zhou, X. Ji, D. Gong, J. Zhou, Z. Li, W. Liu, Cosface: Large margin cosine loss for deep face recognition, in: *Proceedings of the IEEE Conference on Computer Vision and Pattern Recognition*, 2018, pp. 5265–5274.
- [50] Y. Wen, K. Zhang, Z. Li, Y. Qiao, A discriminative feature learning approach for deep face recognition, in: *European conference on computer vision*, Springer, 2016, pp. 499–515.
- [51] X. Zhang, R. Zhao, Y. Qiao, X. Wang, H. Li, Adacos: Adaptively scaling cosine logits for effectively learning deep face representations, in: *Proceedings of the IEEE Conference on Computer Vision and Pattern Recognition*, 2019, pp. 10823–10832.

- [52] L. Dinh, J. Sohl-Dickstein, S. Bengio, Density estimation using real nvp, arXiv preprint arXiv:1605.08803.
- [53] C. Nhan Duong, K. Gia Quach, K. Luu, N. Le, M. Savvides, Temporal non-volume preserving approach to facial age-progression and age-invariant face recognition, in: The IEEE International Conference on Computer Vision (ICCV), 2017.
- [54] A. Liu, R. Tucker, V. Jampani, A. Makadia, N. Snavely, A. Kanazawa, Infinite nature: Perpetual view generation of natural scenes from a single image, in: Proceedings of the IEEE/CVF International Conference on Computer Vision, 2021, pp. 14458–14467.
- [55] I. Danihelka, B. Lakshminarayanan, B. Uria, D. Wierstra, P. Dayan, Comparison of maximum likelihood and gan-based training of real nvps, arXiv preprint arXiv:1705.05263.
- [56] I. Gulrajani, F. Ahmed, M. Arjovsky, V. Dumoulin, A. C. Courville, Improved training of wasserstein gans, in: Advances in neural information processing systems, 2017, pp. 5767–5777.
- [57] D. Yi, Z. Lei, S. Liao, S. Z. Li, Learning face representation from scratch, arXiv preprint arXiv:1411.7923.
- [58] Z. Liu, P. Luo, X. Wang, X. Tang, Deep learning face attributes in the wild, in: Proceedings of International Conference on Computer Vision (ICCV), 2015.
- [59] G. B. Huang, M. Mattar, T. Berg, E. Learned-Miller, Labeled faces in the wild: A database for studying face recognition in unconstrained environments, in: Workshop on faces in 'Real-Life' Images: detection, alignment, and recognition, 2008.
- [60] S. Moschoglou, A. Papaioannou, C. Sagonas, J. Deng, I. Kotsia, S. Zafeiriou, Agedb: the first manually collected, in-the-wild age database, in: Proceedings of the IEEE Conference on Computer Vision and Pattern Recognition Workshops, 2017, pp. 51–59.
- [61] S. Sengupta, J.-C. Chen, C. Castillo, V. M. Patel, R. Chellappa, D. W. Jacobs, Frontal to profile face verification in the wild, in: 2016 IEEE Winter Conference on Applications of Computer Vision (WACV), IEEE, 2016, pp. 1–9.
- [62] X. Huang, S. Belongie, Arbitrary style transfer in real-time with adaptive instance normalization, in: Proceedings of the IEEE International Conference on Computer Vision, 2017, pp. 1501–1510.
- [63] Y. LeCun, The mnist database of handwritten digits, <http://yann.lecun.com/exdb/mnist/>.
- [64] Y. LeCun, L. Bottou, Y. Bengio, P. Haffner, et al., Gradient-based learning applied to document recognition, Proceedings of the IEEE 86 (11) (1998) 2278–2324.

- [65] A. Odena, C. Olah, J. Shlens, Conditional image synthesis with auxiliary classifier gans, in: Proceedings of the 34th International Conference on Machine Learning-Volume 70, JMLR. org, 2017, pp. 2642–2651.
- [66] T. Salimans, I. Goodfellow, W. Zaremba, V. Cheung, A. Radford, X. Chen, Improved techniques for training gans, in: Advances in neural information processing systems, 2016, pp. 2234–2242.